JOURNAL OF AIRCRAFT
Vol. 42, No. 2, March–April 2005

Inviscid Effects of Thin Shear Layers on Four-Vortex Systems

S. J. Hubbard* and A. J. Marquis†
Imperial College of Science, Technology, and Medicine, London, England SW7 2AZ, United Kingdom

The alleviation of the wake vortex hazard by, for example, promoting vortex instability during aircraft landing and takeoff offers the possibility of increased airport capacity for relatively little cost. The interaction of a vortex pair with a thin shear layer using potential flow methods is extended in this paper to shear-layer interactions with more realistic four-vortex systems. Vortex trajectories resulting from encounters with weak and strong shear layers are studied, and the behavior observed is discussed. The effect of the vortex/shear-layer interactions on the robustness of instability mechanisms of four-vortex systems is discussed in relation to the computed trajectories. The computational method enables the salient features of the vortex/shear interactions to be captured in short periods of CPU time using modest processing power. It is concluded that instability mechanisms that utilize the cooperative instability between vortex pairs on either side of the wake are most likely to survive shear-layer interactions.

Nomenclature

b	=	vortex separation
h	=	height of vortex system above shear layer
L	=	periodic wavelength
t	=	time
z	=	position in complex plane
$\bar{z}$	=	complex conjugate of z
Γ	=	circulation
Γ_s	=	circulation of shear-layer vortices
Γ_0	=	reference circulation, $= \lvert\Gamma_1\rvert + \lvert\Gamma_2\rvert$
Δx_s, Δy_s	=	shear-layer vortex spacing in x and y directions, respectively

Subscripts

s	=	shear layer
1	=	outboard vortex pair
2	=	inboard vortex pair

Superscripts

P	=	periodic system
R	=	rigid system
$*$	=	nondimensionalized

I. Introduction

THE behavior of trailing vortices behind aircraft has important implications for the safety and capacity of aircraft and airports. Safety because encounters between aircraft and trailing vortices are highly undesirable, particularly during landing and takeoff although those under cruise conditions, must not be disregarded. The potential for encounters during takeoff and landing determines separations between successive landing and takeoffs, and these separations determine the ultimate capacity of the airport. To shorten these separations, and thus increase capacity, the behavior of trailing vortices under various atmospheric and flight conditions needs to be quantified. In this paper previous work on the interaction of wake vortices and shear layers is developed to include more realistic vortex systems and to explore the effect of the vortex/shear interactions on instability mechanisms.

Atmospheric shear can have significant effects on the behavior of aircraft trailing vortices. Observations of a pair of trailing vortices in a ground shear flow with crosswind show that the upwind vortex usually drops to a lower altitude than the downwind vortex. Burnham,[1] using two-dimensional inviscid theory, a single row of point vortices to represent the ground shear layer and a vortex pair representing the trailing vortices, found that the shear layer was swept up around the downwind vortex, causing its descent to be slowed by the influence of the shear vorticity. Proctor et al.[2] studied the interaction of a thin shear zone with a vortex pair using a two-dimensional large-eddy simulation (LES) approach. The downwind trailing vortex, which has vorticity of opposite sign to the shear layer vorticity, descended less than the trailing vortex of the same sign. Increasing the strength of the shear layer caused the vortex of opposite sign to rebound upward, away from the shear zone. Subsequently, Zheng and Baek[3] proposed that the mechanism responsible for the asymmetric deflections could be deduced from the inviscid interactions between the trailing vortices and the vortices that form the shear layer. The simulations of Zheng and Baek, similar to those of Burnham, represented the shear layer with five rows of vortices and showed that the behavior of the trailing vortices qualitatively reproduced that in the LES simulations of Proctor et al.[2] and the LES and direct numerical simulations of Darracq et al.[4] The impetus of representing the interaction of a pair of trailing vortices with a shear layer using two-dimensional potential theory is the dramatic reduction in the required computation time. Zheng and Baek[3] considered that such simulations would be suitable for making real-time wake vortex predictions, which would be of great use to airport operators who could use the results of predictions to optimise the separation distances between aircraft and increase airport capacity. With this in mind, Zheng and Lim[5] improved the model of Zheng and Baek[3] to include ground effects and vortex decay and validated the predictions against the simulations of Proctor et al.[2] and the measured data of Garodz and Clawson.[6]

The work just described considered the interaction of a vortex pair with a shear layer, either at altitude or near to the ground, and has resulted in good understanding of the physics involved and shows promise for implementation into a real-time wake vortex prediction algorithm.[5] However, it is well known[7] that in the extended near field (∼20–40 wing spans) multiple pairs of trailing vortices are shed from the wing and flap tips at the trailing edge. For a B747, with a wingspan of around 60 m, this corresponds to a distance of 1.2–2.4 km behind the aircraft. Information on the trajectories of multiple vortex pairs as a result of interaction with shear layers is therefore desirable. Four-vortex systems have also received considerable attention because of their instability properties,[8–15] which are

Received 3 November 2003; revision received 14 August 2004; accepted for publication 17 August 2004.

*Ph.D. Student, Department of Mechanical Engineering, Exhibition Road, South Kensington.

†Senior Lecturer, Department of Mechanical Engineering, Exhibition Road, South Kensington.

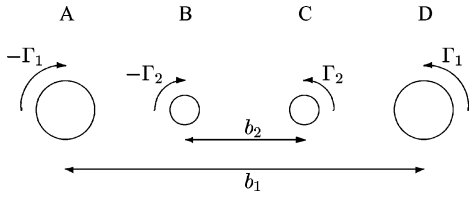

Fig. 1a Four-vortex system.

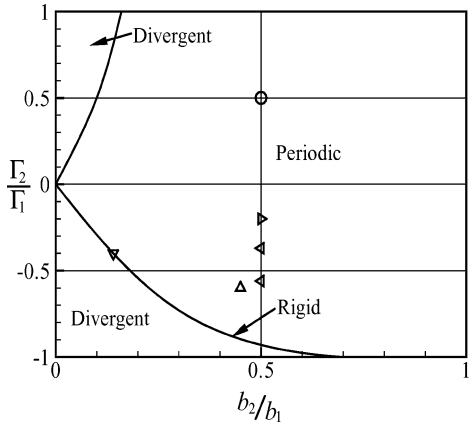

Fig. 1b Classification chart; symbols correspond to the theoretical and numerical work of the following references: ○, Crouch[8]; ▽, Rennich and Lele[9] and Fabre and Jacquin[10]; and △, Quackenbush et al.[11] These symbols corresponds to the experimental measurements of the following references: ▷, Ortega and Savas[13]; and ◁, Ortega et al.[15]

dependent on the spacing and strength ratios of the two pairs. Instabilities of vortex wakes are of interest as they are a prime candidate for wake alleviation schemes that seek to promote early destruction of aircraft wakes. Early destruction is a key enabler to increase the capacity of commercial airports without the construction of new runways. Four-vortex systems show good potential for such an alleviation scheme as the growth rate of the different forms of instability can be orders of magnitude greater[9] than the growth rate of the Crow instability,[16] which occurs on a single vortex pair. A four-vortex system comprising two pairs is shown in Fig. 1a. The outboard vortices Γ_1 are considered to be generated from the wing tips, and the inner vortices Γ_2 from either the outboard edge of a flap in which case they are corotating with the wing-tip vortices and are like signed, or from the inboard edge of a flap in which case they are counter-rotating with the wing-tip vortices and thus of opposite sign. This configuration of vortices was first analyzed in two dimensions by Donaldson and Bilanin,[17] who showed that the evolution of the system is periodic (the two vortices on each side of the wake rotate about their circulation centroid while descending), divergent (the inboard and outboard pairs separate) or rigid (the four vortices retain their relative positions and translate downwards) depending upon the ratios Γ_2/Γ_1 and b_2/b_1. Their classification chart is reproduced in Fig. 1b with additional annotations representing previous stability studies.

The two factors just described have motivated the current study, which will investigate the effect of interactions with a thin shear layer on four-vortex systems initially above the shear zone. Trailing vortex trajectories are computed, using the method of Zheng and Baek,[3] for interactions of periodic and rigid vortex systems with "weak" and "strong" shear layers. The trajectories are then used to qualitatively judge which instability mechanisms are most likely to survive a shear-layer interaction; a quantitative assessment of the growth of the instability mechanisms during the encounter with the shear layer and after is not possible because of the highly three-dimensional nonlinear nature of the trailing vortex wake.

II. Numerical Model

The aircraft wake and the shear layer are modeled as a number of vortices, and in the complex plane $z = x + iy$ the velocity of the pth point vortex of system of N point vortices is given by

$$\frac{\mathrm{d}z_p}{\mathrm{d}t} = \frac{i}{2\pi}\sum_{q\neq p}^{N}\Gamma_q\frac{z_p - z_q}{|z_p - z_q|^2} \tag{1}$$

To remove the end effects of the edges of the shear layer, infinite periodic boundary conditions are applied at the left and right boundaries of the domain.[3] Equation (1) then becomes[18]

$$\frac{\mathrm{d}\bar{z_p}}{\mathrm{d}t} = -\frac{i}{2L}\sum_{q\neq p}^{N}\Gamma_q\cot\frac{\pi(z_p - z_q)}{L} \tag{2}$$

To determine the vortex trajectories, a set of N nonlinear equations of the form (2) must be solved, which can only be achieved by numerical integration. Previous use of Eq. (2) to study shear-layer effects on a single pair of trailing vortices used an Euler integration step[3,5]:

$$\bar{z_p}^{n+1} = \bar{z_p}^{n} + f\,\Delta t \tag{3}$$

where f is the right-hand side of Eq. (2). In the absence of a shear layer, a pair of corotating equistrength point vortices orbit each other about their center point. The use of an Euler scheme to model this behavior introduces an error proportional to the time step at every stage of the computation, which increases the separation of the pair.[19] This is because of the vortex trajectories being tangents to the displacement vector $f\Delta t$. For a counter-rotating equistrength pair, which undergo simple translational motion, Eq. (3) will correctly calculate the motion as the vortex trajectories are coincident with $f\Delta t$. Equation (3) can be used for rotating systems, but the very small time steps needed to reduce the error to acceptable levels make the scheme computationally inefficient. A preferable alternative is to use higher-order integration schemes, such as the fourth-order Runge–Kutta scheme:

$$\bar{z_p}^{n+1} = \bar{z_p}^{n} + \tfrac{1}{6}(f^n + 2f' + 2f'' + f''')\Delta t \tag{4}$$

where

$$f' = f\left(t^{n+\frac{1}{2}}, \bar{z_p'}\right), \qquad \bar{z_p'} = \bar{z_p}^{n} + \tfrac{1}{2}f^n\Delta t \tag{5}$$

$$f'' = f\left(t^{n+\frac{1}{2}}, \bar{z_p''}\right), \qquad \bar{z_p''} = \bar{z_p}^{n} + \tfrac{1}{2}f'\Delta t \tag{6}$$

$$f''' = f\left(t^{n+1}, \bar{z_p'''}\right), \qquad \bar{z_p'''} = \bar{z_p}^{n} + f''\Delta t \tag{7}$$

which samples the velocities at locations in the flowfield in addition to $\bar{z_p}^{n}$. The added reevaluations of the right-hand side of Eq. (2) make the Runge–Kutta scheme computationally expensive, and a careful choice of Δt is needed to obtain an accurate solution in a reasonable amount of CPU time. In this study of four-vortex systems, Eq. (3) will be used for rigid systems and Eq. (4) for periodic systems to keep the CPU requirements low.

III. Results and Discussion

A. Configuration

The four trailing vortices are represented by point vortices, and the shear layer is modeled by five rows of point vortices each of constant strength. In the model configuration shown in Fig. 2, the shear vortices (each of strength Γ_s) have the same sign as vortex A; vortices A (strength Γ_1) and B (strength Γ_2) are called the upwind pair, and C and D are the downwind pair. All distances are normalized by b_1 and circulations by Γ_0, which is defined as $|\Gamma_1| + |\Gamma_2|$. The width of the calculation domain, L in Fig. 2, was chosen so that over the course of the calculation the shear layer at the ends of the calculation domain remained undisturbed, that is, all interactions between the four vortices and the shear layer were confined to the centre of the calculation.

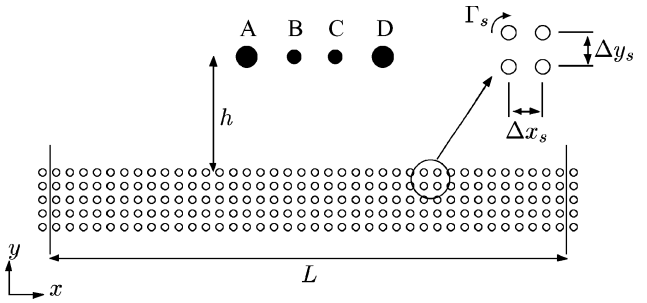

Fig. 2 Numerical model configuration.

1. Shear Layer

Zheng and Baek[3] studied shear layers with $\Gamma_s = 1, 2$, and 10% of the strength of the tip vortices. If an effective shear circulation Γ_{eff} is introduced and defined as

$$\Gamma_{\text{eff}} = \Gamma_s \big/ \Delta x_s^* \Delta y_s^* \tag{8}$$

the calculations of Zheng and Baek employed shear layers with effective circulations of $0.16\Gamma_1$, $0.32\Gamma_1$, and $1.6\Gamma_1$, where Γ_1 was the strength of their tip vortices. In this investigation the reference circulation is given by Γ_0 resulting in comparable shear layers with effective circulations of $\Gamma_{\text{eff}} = 0.16\Gamma_0$ (weak) and $1.6\Gamma_0$ (strong) representing the extremes of those used by Zheng and Baek.

In all cases considered, the shear layer is $0.5b_1$ thick and covers the region $y = b_1 \to 1.5b_1$, that is, $1 \le y^* \le 1.5$. If the wake behind a B747 is considered, this corresponds to a shear-layer thickness of 30 m, which is that used in the studies of Refs. 2 and 4. Preliminary sensitivity studies showed that the vortex trajectories are sensitive to the alignment of the vortices in the x direction when using the values of $\Delta x_s^* = 0.5$ and $\Delta y_s^* = 0.125$ as used by Ref. 3. Reducing Δx_s^* to 0.25 and reducing Γ_s to maintain the value of Γ_{eff} resulted in trajectories that were independent of the alignment of the shear layer in the x direction. Further reduction of Δy_s^* (i.e., increasing the number of rows in the shear layer) has no effect on the vortex trajectories.

2. Vortex Strengths and Starting Location

The vortices are started from rest above the shear layer and descend downwards towards the shear layer. The orientation that the co- and counter-rotating vortices encounter the shear layer is determined by their starting location. In an attempt to ensure that the trajectories obtained with the co- and counter-rotating vortices are comparable with each other, the starting points are located so that, in the absence of the shear layer, the vortices undergo approximately one complete rotation between their starting points and the start of shear layer. To do this, the descent speeds of the vortex systems must therefore be considered.

The descent speed of a rigid system is given by the descent speed of an equivalent vortex pair located at the circulation centroids located on each half of the wake, that is,

$$V_D = (\Gamma_1 + \Gamma_2)/2\pi\tilde{b} \tag{9}$$

where $\tilde{b}$ is the separation between the circulation centroids from each half of the wake $[\tilde{b} = (\Gamma_1 b_1 + \Gamma_2 b_2)/(\Gamma_1 + \Gamma_2)]$. The decent speeds of co- and counter-rotating systems vary periodically during the descent and are dependent on the strength and separation ratios of the system by Ortega (Ref. 20, pp. 35, 36, 38, and 39). In the present study the descent speed, for the purpose of specifying the starting location, of a nonrigid system is approximated by taking the descent speed of an equivalent vortex pair located at the circulation centroids located on each half of the wake, that is, Eq. (9). Rigid systems are time normalized by the time taken for the system to descend a distance b_1:

$$t_0^R = b_1 \big/ V_D^R \tag{10}$$

Periodic systems are time normalized by the orbit period of the vortices on the same side of the line of symmetry. Considering the vortices in one-half of the wake, the orbit period is given by[18]

$$t_0^P = \frac{4\pi^2 (b_1 - b_2)^2}{(\Gamma_1 + \Gamma_2)} \tag{11}$$

The downward distance traveled during one orbit of each of the pairs is approximately

$$d = V_D^P \, t_0^P \tag{12}$$

The initial height above the shear layer is constant for rigid systems, that is, $h = 0.5\, b_1$ but varies for the reason just given for periodic systems and is determined from Eq. (12), that is, $h = d$.

Results for rigid systems with strength ratios $\Gamma_2/\Gamma_1 = -0.1 \to -0.9$, along the curve in Fig. 1b, are presented, along with periodic systems at $\Gamma_2/\Gamma_1 = 0.1, 0.5, 0.9$ for corotating pairs and $\Gamma_2/\Gamma_1 = -0.1, -0.5$ for counter-rotating pairs, between $b_2/b_1 = 0.5$ and the boundary with divergent systems. In the region $b_2/b_1 > 0.5$ the effect of the shear layer on the vortex trajectories diminishes as $b_2/b_1 \to 1$.

The time step and periodic wavelengths used for simulation of the separate regimes are given in Table 1. In all cases the same periodic wavelength as Zheng and Baek[3] was used, with the exception of corotating system interacting with the weak shear layer where it was reduced to save CPU time. This reduction was possible because in this case the vortex trajectories remain close to the center of the domain. Sensitivity studies showed no change in trajectories when L was increased from the values given in Table 1.

The nondimensional simulation time in each case was $1000\Delta t^*$. The computer program was written in C and compiled using Borland C^{++} compiler version 5.02, and calculations were run on an 833-MHz PC with 128 Mbyes of memory running Windows-NT.

Table 1 Simulation details

Regime	Shear layer	L/b_1	Δt^*	Integration method	CPU time
Rigid	Weak	20.25	0.01	Euler	460 s
	Strong	20.25	0.01	Euler	460 s
Corotating	Weak	10.25	0.005	Runge–Kutta	500 s
	Strong	20.25	0.005	Runge–Kutta	1600 s
Counter-rotating	Weak	20.25	0.005	Runge–Kutta	1600 s
	Strong	20.25	0.005	Runge–Kutta	1600 s

B. Rigid Systems

The computed trajectories of the four vortices during interaction with a weak shear layer ($\Gamma_{\text{eff}} = 0.16\Gamma_0$) are shown in Fig. 3 for varying strength ratios [the associated initial separation ratio (b_2/b_1) were determined from Fig. 1b]. At low strength ratios ($\Gamma_2/\Gamma_1 = -0.1$) the inboard vortices interact strongly with each other and weakly with the left-most tip vortex, while the right-most vortex is undisturbed. As the strength ratio increases to $\Gamma_2/\Gamma_1 = -0.5$, the upwind pair interacts strongly while the downwind pair appears to undergo no interaction with each other. As Γ_2/Γ_1 increases further, the level of interaction between the upwind pair diminishes, and a weak interaction was found to occur on the downwind pair for $\Gamma_2/\Gamma_1 = -0.9$ (not shown). Rigid systems are very sensitive to perturbations of the positions of any of the four vortices, as this will result in a change in b_2/b_1, moving the system into either the periodic or divergent regimes. For low b_2/b_1, the inboard vortices are very close to each other and are both perturbed in the same way, that is, they are displaced toward the tip vortex of same circulation sign as the shear layer (A in this case), and both become entrained around it (Fig. 3a). As b_2/b_1 increases, the perturbation to B causes it to interact strongly with A while C is moved further away from D resulting in little interaction. Increasing b_2/b_1 further has a less dramatic effect as the perturbations on B and C affect the pair on each half of the wake rather than simply moving B or C towards A. This behavior can be explained through consideration of how strongly coupled the vortex pairs in each half of the wake are. Consider a vortex pair with ($\Gamma_2/\Gamma_1 \ll 1$),

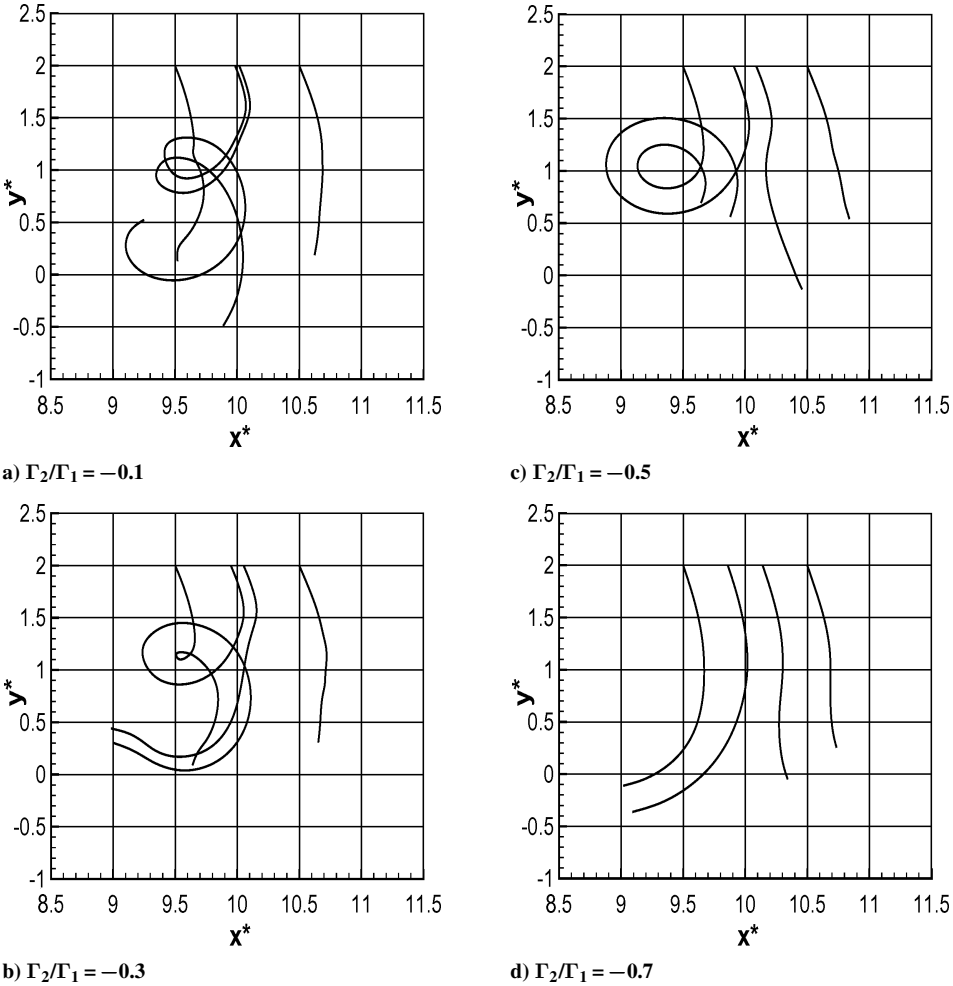

a) $\Gamma_2/\Gamma_1 = -0.1$ c) $\Gamma_2/\Gamma_1 = -0.5$

b) $\Gamma_2/\Gamma_1 = -0.3$ d) $\Gamma_2/\Gamma_1 = -0.7$

Fig. 3 Rigidly translating four-vortex systems of varying circulation and shear layer ($\Gamma_{\text{eff}} = 0.16\Gamma_0$).

any perturbation to the strong vortex will have a greater effect on the position of the weak vortex than a perturbation to the weak vortex will have on the stronger one, because of the difference in intensity of the induced velocity fields. A vortex pair with $(\Gamma_2/\Gamma_1 \approx 1)$ is thus strongly coupled, whereas a pair with $(\Gamma_2/\Gamma_1 \ll 1)$ is weakly coupled. It is therefore relatively easy for the weaker vortex in a weakly coupled pair to be separated from the stronger vortex. This is why the inboard pair become easily separated from the outboard pair when the strength ratio is low. Similar arguments can be made showing that a vortex pair with lower separation is more strongly coupled than a pair that is further apart.

Figure 4 shows the trajectories during interactions with a strong shear layer ($\Gamma_{\text{eff}} = 1.6\Gamma_0$). In contrast to the interaction with the weak shear layer above the interaction of the vortex system with the strong shear layer results in one, two, or three of the vortices rebounding depending on the strength and separation ratios of the vortex pairs; a low strength ratio results in the downwind tip vortex only experiencing rebound, while from $\Gamma_2/\Gamma_1 = -0.5$ and above the upwind tip vortex is the only one not to experience rebound.

Zheng and Baek[3] found that in the case of a pair of counter-rotating vortices the downwind vortex (with opposite sign to the shear vortices) sweeps some of the shear layer around it, which then induces an upward velocity on it, causing it to rebound. In the case of a four-vortex rigid system, the downwind tip vortex (vortex D) behaves in the same way; it always rebounds. Indeed the upwind vortex (A) always penetrates the shear layer, as does its counterpart in a single counter-rotating pair.[3] The behavior of vortices B and C can be explained in the same way as for the interaction with weak shear layers. For low b_2/b_1 (=0.1) both B and C are entrained around A and hence penetrate the shear layer. As b_2/b_1 increases, C is no longer entrained around A and is caught up in the roll up of the shear layer on the downstream side of the wake. (The shear layer has in effect been split, and so each half rolls up at its end in the middle of the wake.) As b_2/b_1 increases further, vortex B is also caught up in the roll up of the split shear layer and so rebounds along with C and D.

C. Corotating Periodic Systems

Figures 5–7 show the vortex trajectories for corotating systems of strength ratios $\Gamma_2/\Gamma_1 =$ 0.1, 0.5, and 0.9, respectively, interacting with a weak shear layer and Fig. 8 a corotating system of strength ratio $\Gamma_2/\Gamma_1 =$ 0.5 interacting with a strong shear layer.

Figure 6 shows that for a corotating system with $\Gamma_2/\Gamma_1 = 0.5$ and $b_2/b_1 = 0.2 \rightarrow 0.5$ all of the vortices pass through the shear layer. For high b_2/b_1 the vortex pairs rotate about each other with only slight changes to their trajectory (Fig. 6d). As b_2/b_1 decreases, the orbit period and orbit radius of the vortex pair with the same sign as the shear (upwind pair in this case) increase as a result of the shear layer accelerating the upwind pair in the downward direction and decelerating the downwind pair. For low b_2/b_1 (= 0.2) the orbit radius of the like signed upwind pair is increased to such an extent that the weaker inboard vortex is entrained around the stronger tip vortex from the opposite side of the wake (Fig. 6a); once this happens the periodic nature of the system is disrupted.

The general trends observed for a circulation ratio of 0.5 are also observed for ratios below, that is, 0.1 (Fig. 5) and above, that is, 0.9 (Fig. 7). As the separation ratio b_2/b_1 approaches, the critical divergence value (the solid line in the top half of Fig. 1b), the orbit period, and radius of the upwind pair are increased. For the higher strength ratio ($\Gamma_2/\Gamma_1 = 0.9$) an increase of orbit radius and orbit period occurs when the separation ratio is closer to the critical

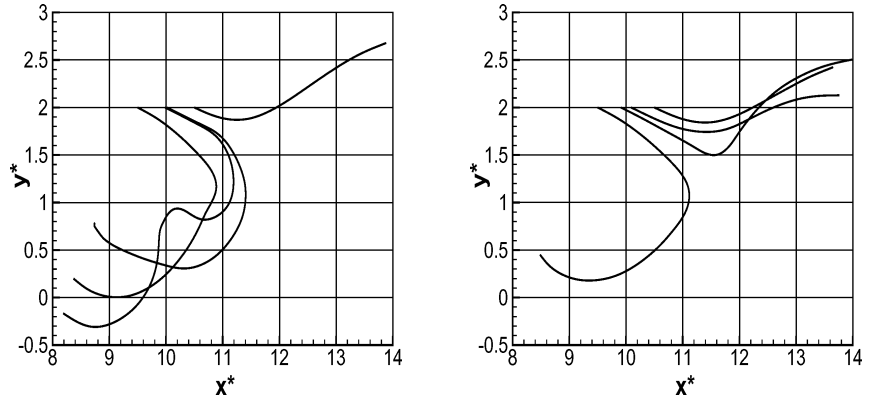

a) $\Gamma_2/\Gamma_1 = -0.1$ c) $\Gamma_2/\Gamma_1 = -0.5$

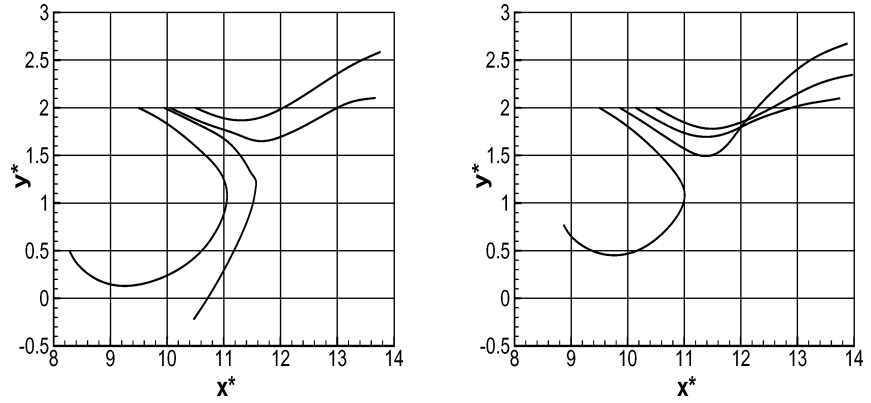

b) $\Gamma_2/\Gamma_1 = -0.3$ d) $\Gamma_2/\Gamma_1 = -0.7$

Fig. 4 Rigidly translating four-vortex systems of varying circulation and shear layer ($\Gamma_{\text{eff}} = 1.6\Gamma_0$).

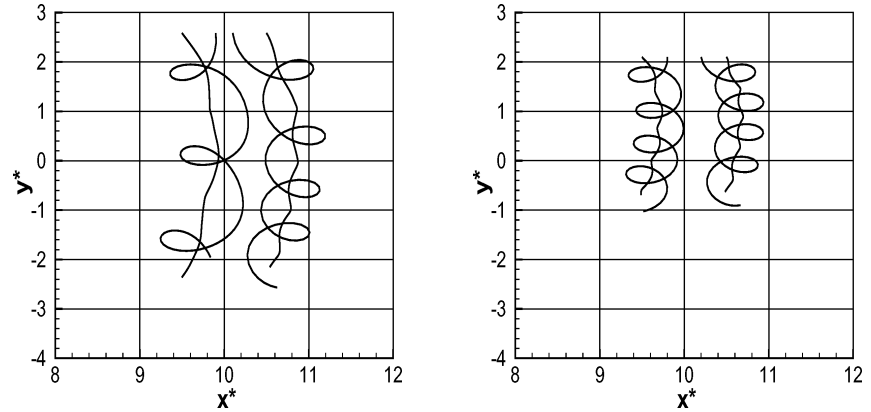

a) $b_2/b_1 = 0.2$ c) $b_2/b_1 = 0.4$

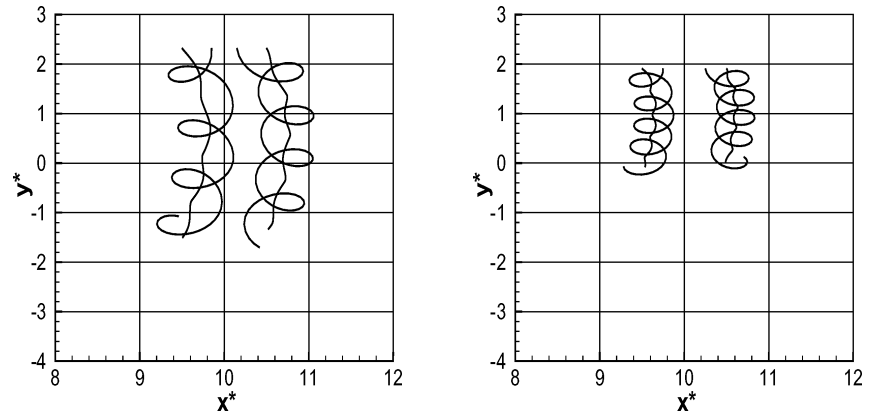

b) $b_2/b_1 = 0.3$ d) $b_2/b_1 = 0.5$

Fig. 5 Corotating periodic system ($\Gamma_2/\Gamma_1 = 0.1$) with varying separation ratio and shear layer ($\Gamma_{\text{eff}} = 0.16\Gamma_0$).

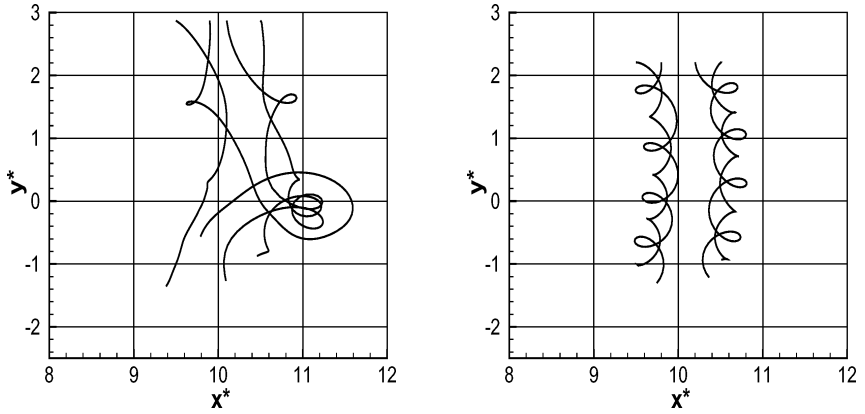

a) $b_2/b_1 = 0.2$ c) $b_2/b_1 = 0.4$

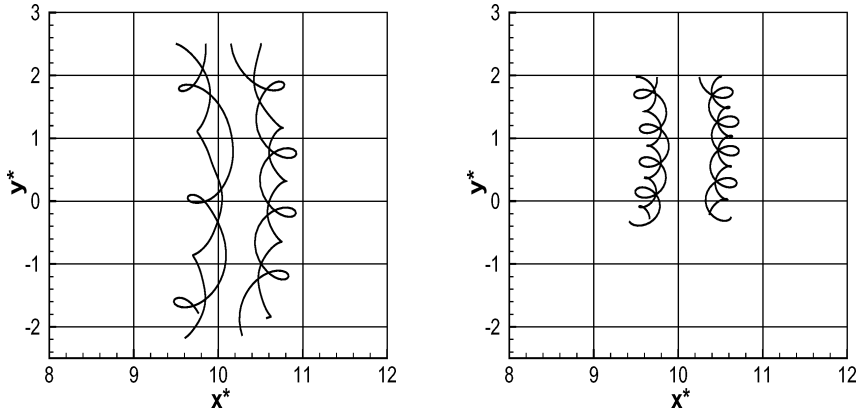

b) $b_2/b_1 = 0.3$ d) $b_2/b_1 = 0.5$

Fig. 6 Corotating periodic system ($\Gamma_2/\Gamma_1 = 0.5$) with varying separation ratio and shear layer ($\Gamma_{\text{eff}} = 0.16\Gamma_0$).

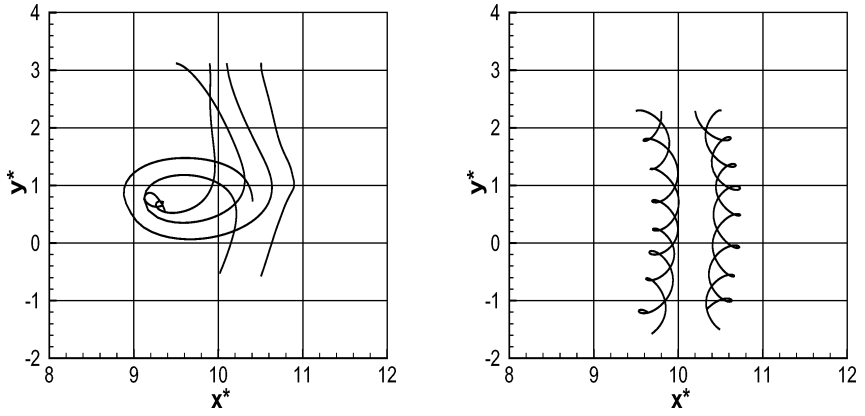

a) $b_2/b_1 = 0.2$ c) $b_2/b_1 = 0.4$

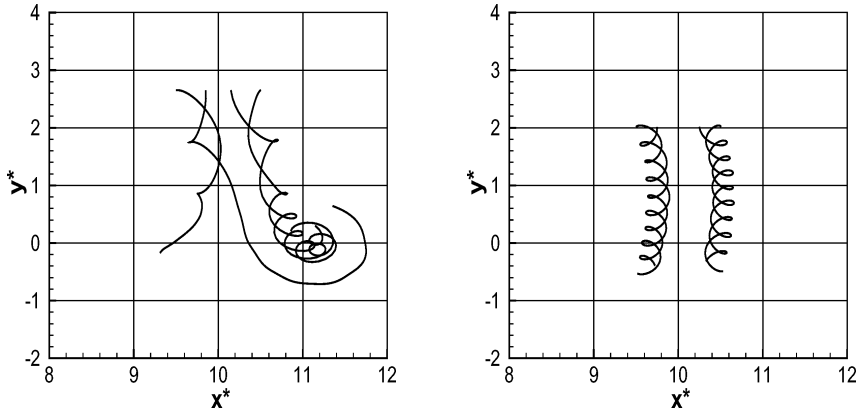

b) $b_2/b_1 = 0.3$ d) $b_2/b_1 = 0.5$

Fig. 7 Corotating periodic system ($\Gamma_2/\Gamma_1 = 0.9$) with varying separation ratio and shear layer ($\Gamma_{\text{eff}} = 0.16\Gamma_0$).

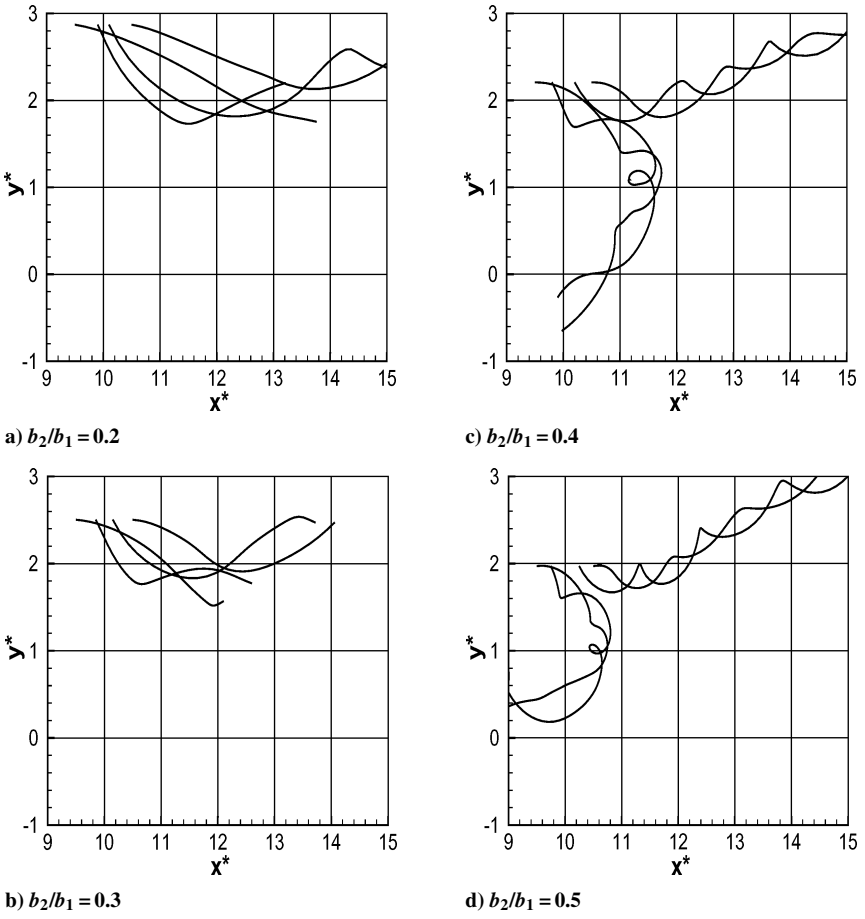

Fig. 8 Corotating periodic system ($\Gamma_2/\Gamma_1 = 0.5$) with varying separation ratio and shear layer ($\Gamma_{eff} = 1.6\Gamma_0$).

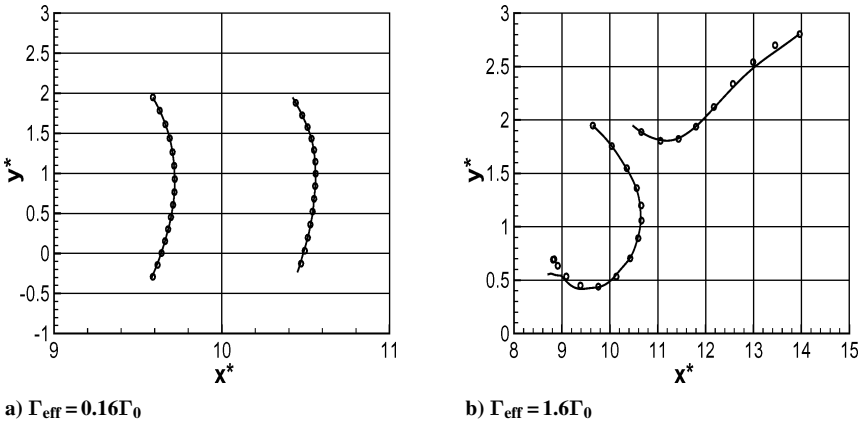

Fig. 9 Trajectory of circulation centroid of strongly coupled corotating four-vortex systems compared with trajectory of single vortex pair of equivalent strength placed at centroid location: ——, centroid from each side of four vortex wake; ○, locations of equivalent vortex pair.

divergence value than for $\Gamma_2/\Gamma_1 = 0.1$. In the cases with a high separation ratio, the trajectory of the upwind and downwind pairs can be modeled by considering a single vortex pair located at the circulation centroids on each half of the wake of the four-vortex system with strengths Γ_0. The trajectory of the vortex pair is identical to the path of the circulation centroids on each half of the four vortex system, as shown in Fig. 9a.

Figure 8 shows the behavior of systems with $\Gamma_2/\Gamma_1 = 0.5$ and varying b_2/b_1 for interactions with a strong shear layer. For low b_2/b_1 all four vortices remain above the shear layer for the duration of the simulations; the graphs have been cut short as a result of the individual trajectories becoming indistinguishable a short time into the simulations. Not shown in the figure, the vortices "bounce" along the top of the shear layer. Both the rotating influence of the outboard vortices and the influence of each other accelerates the inboard vortices of each pair downward. They interact with the shear layer before the outboard vortices (because of the initial condition $h = d$), and the inboard vortex of opposite sign to the shear layer (vortex C) sweeps up a region of the shear layer as in the classic rebound mechanism described earlier. This sweeping process causes the shear layer to split as in the case just described, and the separated ends roll up in the classical way, as shown in Fig. 10a. All four vortices are caught up in the roll up of the right-hand side of the shear layer and remain above it. In the latter stages of the simulation, the rolling up of the shear layer progresses towards the periodic boundary and loses its identity; study of the

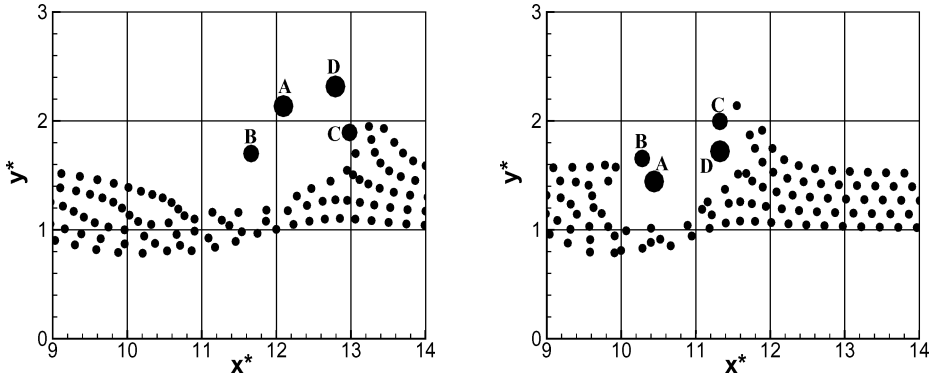

a) $b_2/b_1 = 0.2$ b) $b_2/b_1 = 0.5$

Fig. 10 Different interactions of corotating system with $\Gamma_2/\Gamma_1 = 0.5$ with a shear layer of $\Gamma_{\text{eff}} = 1.6\Gamma_0$ at $t^* = 0.08$.

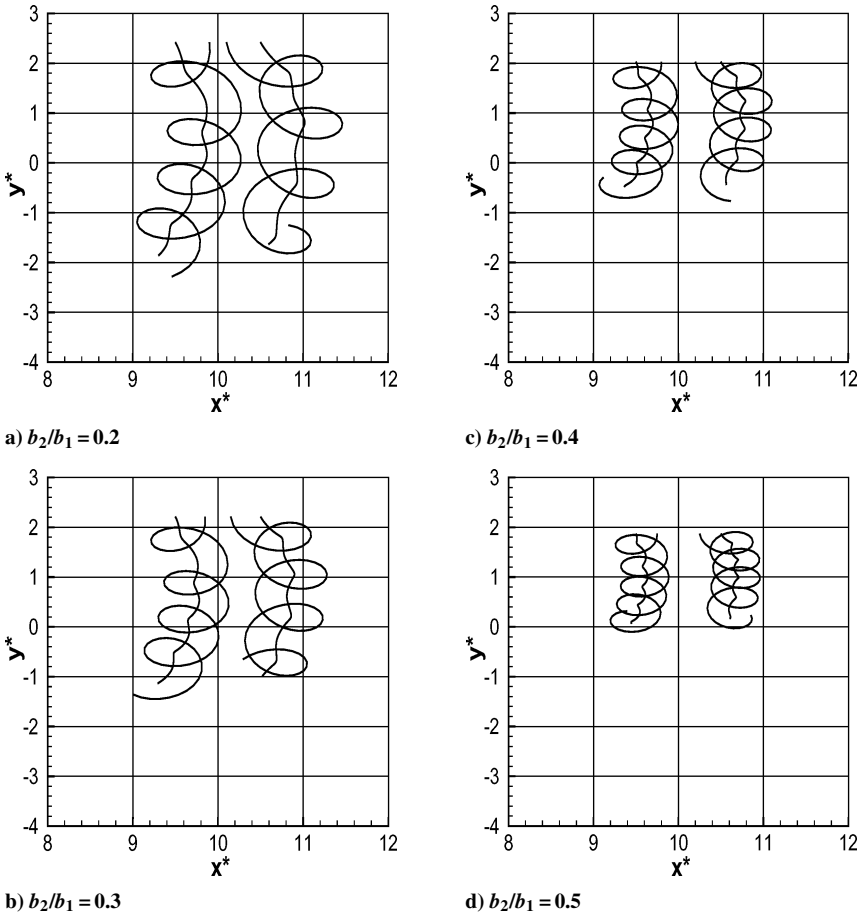

a) $b_2/b_1 = 0.2$ c) $b_2/b_1 = 0.4$

b) $b_2/b_1 = 0.3$ d) $b_2/b_1 = 0.5$

Fig. 11 Counter-rotating periodic system ($\Gamma_2/\Gamma_1 = -0.1$) with varying separation ratio and shear layer ($\Gamma_{\text{eff}} = 0.16\Gamma_0$).

long-term evolution will require specification of a larger L than used here. In the context of the present study, the key behavior, that is, the splitting of the vortex system, is obtained at early evolution times.

Increasing the separation ratio reduces the orbit period of the vortices on each half of the wake; the two inboard vortices do not interact with the shear layer significantly before the outboard vortices, and so vortex C does not sweep up shear vorticity on its own. Rather the downstream pair sweep up shear vorticity together as shown in Fig. 10b. The upstream pair is strongly coupled and penetrates the shear layer together. As b_2/b_1 increases, the pairs on either side of the wake become more strongly coupled, and the trajectory of the centroids tends toward the trajectory of a single vortex pair of strength and location equal to the centroid of the four-vortex system, as shown in Fig. 9b. Similar behavior was observed for all strength ratios considered; for $b_2/b_1 < 0.4$ the four vortices all rebound, whereas for $b_2/b_1 \geq 0.4$ the upwind pair penetrates the layer while the downwind pair rebounds.

D. Counter-Rotating Periodic Systems

Figure 11 shows the trajectories of the vortices with $\Gamma_2/\Gamma_1 = -0.1$ for interactions with a weak shear layer. For all b_2/b_1, all four vortices proceed through the shear layer without any separations—the two pairs remain separate and distinct. The difference between the co- and counter-rotating case (Figs. 5 and 11, respectively) is that in the counter-rotating case the downwind pair experiences an increase in orbit period and orbit radius for low b_2/b_1 (as opposed to the upwind pair in the co-rotating case). Figure 12 shows that the trajectories are markedly different for higher Γ_2/Γ_1—the center of rotation has moved further outboard of the tip vortices. For a strength ratio of $\Gamma_2/\Gamma_1 = -0.5$, the downwind pair experiences a

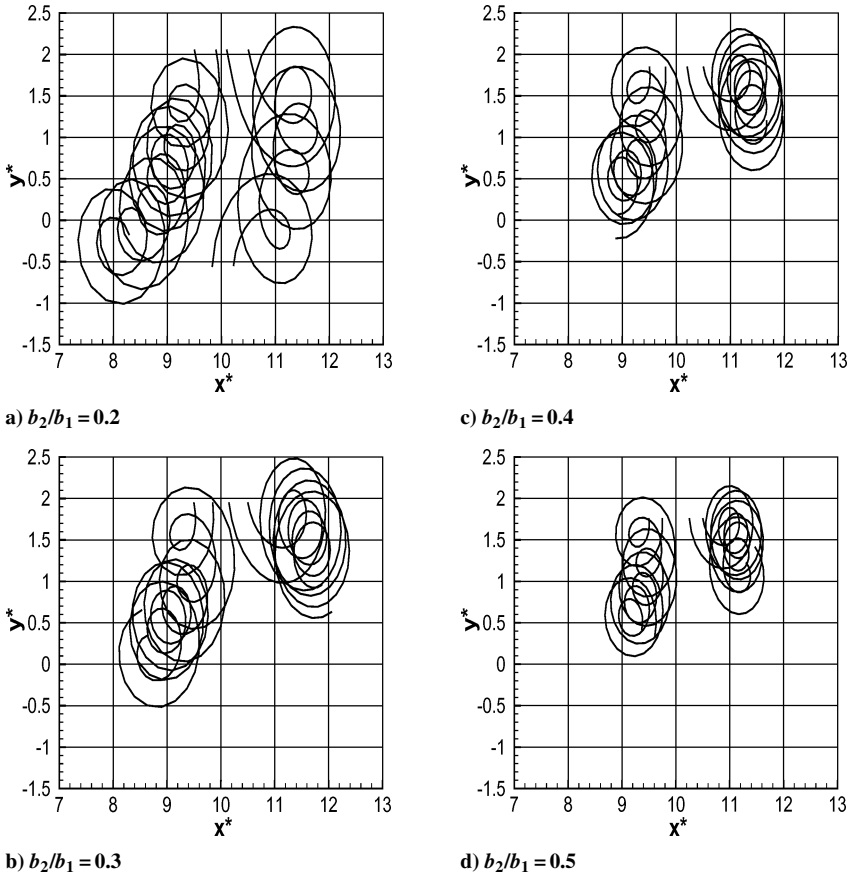

Fig. 12 Counter-rotating periodic system ($\Gamma_2/\Gamma_1 = -0.5$) with varying separation ratio and shear layer ($\Gamma_{eff} = 0.16\Gamma_0$).

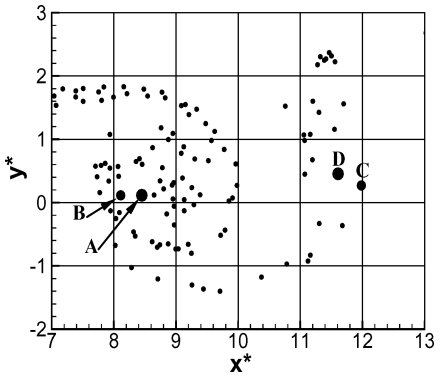

Fig. 13 Interaction of counter-rotating system with $\Gamma_2/\Gamma_1 = -0.5$ with a shear layer of $\Gamma_{eff} = 0.16\Gamma_0$ at $t^* = 0.325$.

dramatic decrease in orbit period, which is greater for lower b_2/b_1 (Figs. 12a–12d). This effect is caused by the vortices disturbing the shear layer as they pass through with a significant amount of the shear vorticity being located near the center of rotation of the vortex pair. The same process occurs on the downwind pair, although less shear vorticity is located near the center of rotation, as shown in Fig. 13. The shear vorticity located near the center of rotation of the upwind pair accelerates the rotation of the vortex pair, whereas for the downwind pair the shear vorticity decelerates the pair. Also, the separation between the upwind pair is reduced during the interaction, increasing the rotation rate of the pair. These effects diminish with increasing separation ratio.

Different strength ratios have a significant effect on vortex trajectories when considering interaction with a strong shear layer. For $\Gamma_2/\Gamma_1 = -0.1$ the behavior of the counter-rotating four-vortex system is the same as for the corotating system; when $b_2/b_1 < 0.4$, all four vortices bounce along the top of the shear layer, and when $b_2/b_1 \geq 0.4$ the pairs on either side of the wake behave like the interaction of single vortices with the downwind pair rebounding and the upwind pair penetrating the shear layer (not shown). For $\Gamma_2/\Gamma_1 = -0.5$ the behavior of co- and counter-rotating systems is very different, as can be seen by comparing Figs. 8 and 14. For counter-rotating systems with $b_2/b_1 = 0.2$, the downwind pair both rebound but then separate, while the upwind pair penetrate the shear layer. As b_2/b_1 increases, the downwind pair always separate with vortex C becoming entrained by the upwind pair. For high b_2/b_1 the pairs are strongly coupled and behave like a single pair with the same centroid behavior as discussed earlier.

E. Effect on Instability Mechanisms

Although the three-dimensional nonlinear nature of the instability mechanisms is not captured in the two-dimensional numerical method used here, it is still possible to draw qualitative conclusions on the ability of the mechanism to grow from the relative trajectories of the four vortices. The mechanism proposed by Rennich and Lele[9] relies on an instability growing on the inboard pair of a rigid system, which subsequently imparts a perturbation that grows on the outboard pair; the four vortices remaining in the rigid configuration and translating downwards together is thus crucial. All interactions of rigid systems with shear layers, with the exception of $b_2/b_1 > 0.8$ when interacting with a weak layer, result in the separation of the pairs from each half of the wake, which would suggest that the mechanism of Rennich and Lele will not lead to vortex destruction in the majority of cases or at best be seriously impaired.

The mechanism described by Crouch[8] was derived for the case of corotating pairs, which translate down at a constant velocity. This instability requires that the four vortices continue to remain in this configuration and do not separate as in the case of the mechanism of Rennich and Lele. Crouch's analysis studied $\Gamma_2/\Gamma_1 = 0.5$, $b_2/b_1 = 0.5$. Under these conditions an interaction with a weak shear layer alters the trajectory of the circulation centroid only slightly and

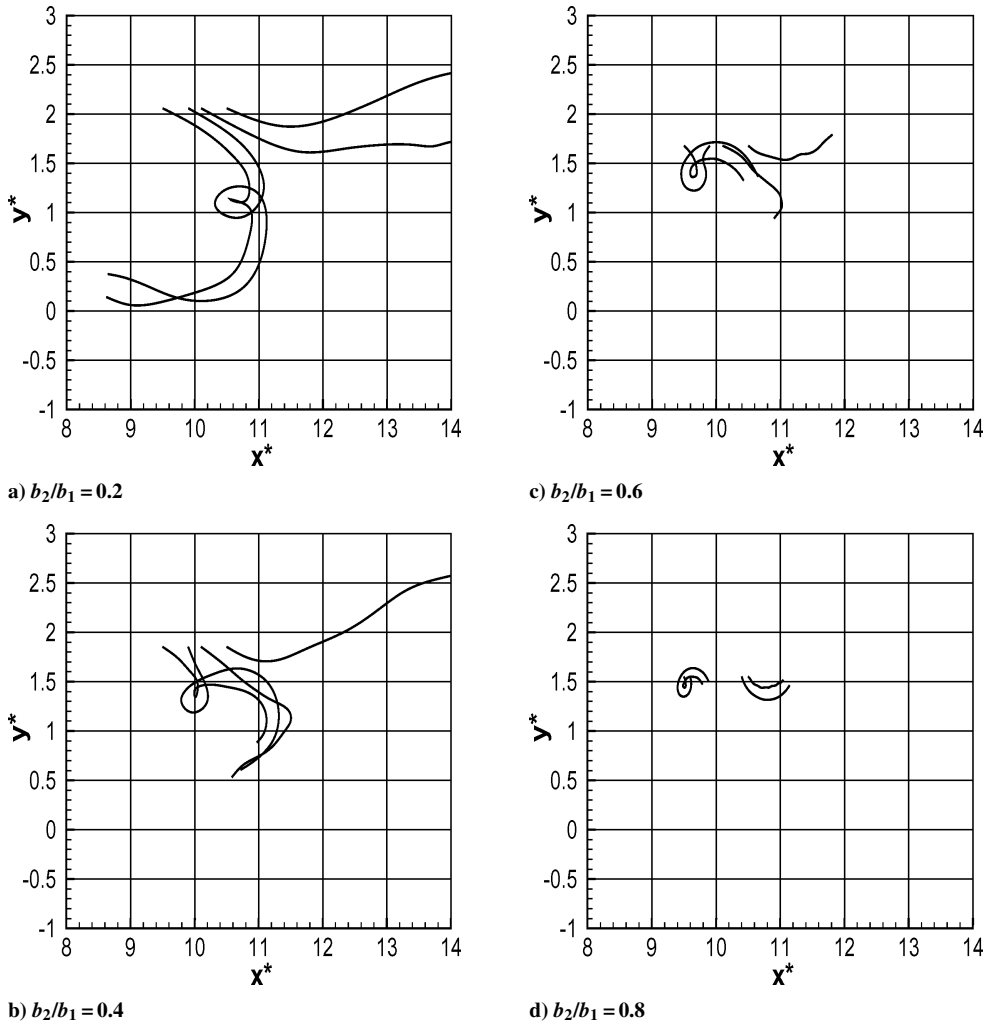

Fig. 14 Counter-rotating periodic system ($\Gamma_2/\Gamma_1 = -0.5$) with varying separation ratio and shear layer ($\Gamma_{eff} = 1.6\Gamma_0$).

does not affect the rotation of the vortices. In this case the interaction with a shear layer will have little effect on the instability mechanism. Strong shear-layer interactions however separate the pairs on each half of the wake and will result in the mechanism having little or no effect.

The mechanism of Quackenbush et al.,[11] Ortega and Savas[13] and Ortega et al.[15] relies only on interaction between the vortices in each half of the wake, that is, the presence of the downwind pair does not affect the upwind pair and vice versa. This mechanism is linked to the short-wavelength instability on a nonrotating pair[21] (for a brief explanation, see Ortega et al.[15]). This mechanism has an advantage over the others with regard to shear-layer interactions because in nearly all cases the pairs on each half of the wake remain together.

One can therefore conclude that instability mechanisms which rely only on interaction between vortices on each half of the wake are most likely to survive an encounter with a shear layer. This view of shear effects on instability mechanisms considers the resultant separation of the vortices as the only means of affecting the instability mechanisms; in reality there can be additional effects.

IV. Conclusions

The interaction of four-vortex systems with thin shear layers has been modeled using point vortices, and several mechanisms explaining the resultant trajectories have been described. The main findings of this study can be summarized as follows:

1) Rigidly translating systems are easily perturbed by weak and strong shear layers, that is, during all shear-layer interactions rigid systems did not retain their original structure.

2) For separation and strength ratios far from the divergent regime, the trajectory of periodic systems is well modeled by simulating the interaction of a single vortex pair representing the circulation centroids.

3) For ratios nearer the divergent regime, periodic systems interacting with shear layers experience an increase in the orbit period and radius on one of the vortex pairs; the upwind pair in corotating systems and the downwind pair in counter-rotating systems.

4) Instability mechanisms that utilize the cooperative instability between vortex pairs on either side of the wake are most likely to survive shear-layer interactions.

This study has used an efficient computational method to explore the behavior of four-vortex systems encountering a shear layer. The method is easily extendable to six or more vortex pairs to simulate the complex vortex structure resulting from multiple flaps and landing gear. Before utilizing the method for more complex flows, the effects of the initial orientation of the vortex system with the shear layer and the thickness of the shear layer should be investigated and the method compared with predictions from Navier–Stokes-based solution procedures.

References

[1]Burnham, D. C., "Effect of Ground Wind Shear on Aircraft Trailing Vortices," *AIAA Journal*, Vol. 10, No. 8, 1972, pp. 1114, 1115.

[2]Proctor, F. H., Hinton, D. A., Han, J., Schowalter, D. G., and Lin, Y. L., "Two Dimensional Wake Vortex Simulations in the Atmosphere: Preliminary Sensitivity Studies," AIAA Paper 97-0056, Jan. 1997.

[3]Zheng, Z. C., and Baek, K., "Inviscid Interactions Between Wake Vortices and Shear Layers," *Journal of Aircraft*, Vol. 36, No. 2, 1999, pp. 477–480.

[4]Darracq, D., Moet, H., and Corjon, A., "Effects of Crosswind Shear and Atmospheric Stratification on Aircraft Trailing Vortices," AIAA Paper 99-0985, Jan. 1999.

[5]Zheng, Z. C., and Lim, S. H., "Validation and Operation of a Wake Vortex/Shear Interaction Model," *Journal of Aircraft*, Vol. 37, No. 6, 2000, pp. 1073–1078.

[6]Garodz, L. J., and Clawson, K. L., "Vortex Wake Characteristics of B757-200 and B767-200 Aircraft Using the Tower Fly-by Techniques. Environmental Research Lab.," Air Resources Lab., National Oceanic and Atmospheric Administration, Rept. 199, Idaho Falls, ID, 1993.

[7]Rossow, V. J., "Wake Hazard Alleviation Associated with Roll-Oscillations of Wake Generating Aircraft," *Journal of Aircraft*, Vol. 23, No. 6, 1986, pp. 484–491.

[8]Crouch, J. D., "Instability and Transient Growth for Two Trailing-Vortex Pairs," *Journal of Fluid Mechanics*, Vol. 350, 1997, pp. 311–330.

[9]Rennich, S. C., and Lele, S. K., "Method for Accelerating the Destruction of Aircraft Wake Vortices," *AIAA Journal*, Vol. 36, No. 2, 1999, pp. 398–404.

[10]Fabre, D., and Jacquin, L., "Stability of a Four-Vortex Aircraft Wake Model," *Physics of Fluids*, Vol. 12, No. 10, 2000, pp. 2438–2443.

[11]Quackenbush, T., Bilanin, A., Batcho, P., McKilipp, R., and Carpenter, B., "Implementation of Wake Vortex Control Using SMA-Actuated Devices," *Proceedings of the SPIE*, edited by J. M. Sater, Vol. 3044, SPIE, Bellingham, WA, 1997, pp. 134–146.

[12]Fabre, D., Jacquin, L., and Loof, A., "Optimal Perturbations in a Four-Vortex Aircraft Wake in Counter-Rotating Configuration," *Journal of Fluid Mechanics*, Vol. 451, 2002, pp. 319–328.

[13]Ortega, J. M., and Savas, Ö., "Rapidly Growing Instability Mode in Trailing Multiple-Vortex Wakes," *AIAA Journal*, Vol. 39, No. 4, 2001, pp. 750–754.

[14]Crouch, J. D., Miller, G. D., and Spalart, P. R., "Active-Control System for Breakup of Airplane Trailing Vortices," *AIAA Journal*, Vol. 39, No. 12, 2001, pp. 2374–2381.

[15]Ortega, J. M., Bristol, R. L., and Savas, Ö., "Wake Alleviation Properties of Triangular-Flapped Wings," *AIAA Journal*, Vol. 40, No. 4, 2002, pp. 709–721.

[16]Crow, S. C., "Stability Theory for a Pair of Trailing Vortices," *AIAA Journal*, Vol. 8, No. 12, 1970, pp. 2172–2179.

[17]Donaldson, C. duP., and Bilanin, A. J., "Vortex Wakes of Conventional Aircraft," AGARDograph No. 204 AGARD-AG-204, Research and Technology Organisation, 1975.

[18]Lamb, H., *Hydrodynamics*, 6th ed. (re-issue), Cambridge Univ. Press, 1974, Chap. 4.

[19]Moore, D. W., "A Numerical Study of the Roll-Up of a Finite Vortex Sheet," *Journal of Fluid Mechanics*, Vol. 63, Pt. 2, 1974, pp. 225–235.

[20]Ortega, J. M., "Stability Characteristics of Counter-Rotating Vortex Pairs in the Wake of Triangular-Flapped Airfoils," Ph.D. Dissertation, Univ. of California, Berkeley, 2001, pp. 35, 36, 38, 39.

[21]Widnall, S. E., Bliss, D. B., and Tsai, C. Y., "The Instability of Short Waves on a Vortex Ring," *Journal of Fluid Mechanics*, Vol. 66, 1974, p. 35.